

Integrated sensors and microsystems

F.J. Ramirez-Fernandez, W.J. Salcedo, and N. Peixoto

*Laboratório de Microeletrônica, Escola Politécnica - Universidade de São Paulo,
05508-900 São Paulo, Brazil.*

Artículo invitado

This work presents a brief review and some significant results about integrated sensors and microsystems such as microelectrode array (MEA) for biological cell culture studies and gas sensors based on nanostructured materials such as porous silicon (PS). Developed MEA provides electrical access to biological neuron culture for signal recording and stimulation showing that the charge injection limit can be lowered to less than 100 nC/cm^2 . The gas sensors based on PS material are investigated using the changes in optical material properties as a function of gas species and concentrations.

Keywords: Integrated sensors; microsystems; porous silicon.

Este trabajo presenta una breve revisión y algunos resultados significativos relacionados al desarrollo de sensores integrados y microsistemas que incluyen, mas que no se limitan a una Matriz de microelectrodos para aplicaciones biológicas en el estudio de cultura de células y aplicaciones del silicio poroso como sensores de gas. La Matriz de microelectrodos permite el acceso eléctrico a la cultura de neuronas para registrar las señales de respuesta a estímulos eléctricos, mostrando que el límite de inyección puede ser disminuido a menos que 100 nC/cm^2 . Los sensores de gas fabricados con silicio poroso son investigados por medio de las variaciones de las propiedades ópticas relacionadas a la concentración y especie de gas.

Descriptores: Sensores integrados; microsistemas; silicio poroso.

PACS: 07.07.Df

1. Introduction

Microelectrode arrays (MEAs) have been used for the last three decades in the field of cellular biology as tools for probing electrophysiologic activity either *in vitro* or *in vivo*. The availability and development of microelectromechanical systems (MEMS) techniques has made possible the fabrication of three dimensional structures which add spatial resolution and cell development control [1-2]. Moreover, the miniaturization of sensors that can be implemented along with the electrodes, such as temperature and pH sensors, makes possible the production of microsystems which will eventually bypass biomedical equipment and provide enough data to define neuronal activity and system status.

Although a high control of neuronal systems is desirable, a high connectivity and, therefore, complexity of neuronal networks makes it very difficult to analyse the amount of data available from such systems. Simplification of neuronal networks that can be isolated, maintained or even formed *in vitro* with a limited quantity of neurons has proven useful for understanding transfer functions and describing basic characteristics of circuits such as pattern generators or rhythmic activity [3]. Such neuronal networks can also be used as sensors for environmental conditions or drug influence on the whole organism. The first step towards such systems is the analysis of cellular adhesion and growth over micromachined substrates, which can then be further developed with onboard circuitry and electrodes. We present here the results of the electrical stimulation of *Helix aspersa* neurons in culture on microelectrode arrays.

2. Microelectrode array fabrication

Planar microelectrode arrays containing 100 electrodes were fabricated as previously reported [4]. Briefly, metal tracks are photolithographically defined on a glass substrate; passivation is either a duplex layer of ECR silicon nitride followed by PECVD thick oxide or polyimide (PI 2525, HD Microsystems). Individual electrodeposition of platinum black on electrodes is performed in order to obtain ohmic impedance below 50 k (at 1 kHz, sinusoidal excitation wave). Alternatively, electrodes are coated with a conductive polymer (polyaniline or polypyrrole) in order to ensure stability during experimental conditions [4]. Medium and long-term (from 10 hours to 10 days) characterization is performed in order to probe electrode stability. The electrode-electrolyte interface has not been modified either by means of mechanical movement or variation of the chemical composition of the electrolyte.

3. Signal recording and stimulation

Computer controlled acquisition and stimulation is performed by means of virtual instrumentation developed with LabVIEW®. Signal acquisition can be performed on 32 channels differentially and input levels are set according to the signal variation observed during the experiment. Upon identification of the active electrodes, a maximum of four sites are chosen and saved for subsequent analysis. Cells placed over the electrodes can be visually identified and respectively accessed by means of differential recording from neighbouring electrodes. Stimulation threshold for isolated

cells is then probed by applying charge balanced square pulses in trains between electrodes, which are arranged across the cell body. The threshold is defined as the electrical stimulus that repeatedly elicits extracellular action potentials for each of the applied pulses. The current profile depends on the electrode impedance and seal to the cell. The charge injection threshold is found to be $0.08 \mu\text{C}/\text{cm}^2$. Depending on the time in culture, the threshold can vary by one order of magnitude. Nevertheless, this value is much lower than the threshold usually found for neural implants, such as the retinal [5], due to the controlled environment. The determination of the lower baseline for neural prosthesis can then start by looking at some cultured cell thresholds. We were also able to inhibit neuronal activity by means of electrical stimulation (unidentified neurons from the parietal ganglion). In this case, the spontaneous activity is in the range of 4 to 12 spikes/s. As soon as the stimulus sequence begins, the activity is completely depressed, showing the inhibitory effect observed in roughly 20% of the unidentified neurons maintained in culture for more than 10 days.

Threshold is considered to be the electrical stimulus which repeatedly elicits extracellular action potentials for each of the applied pulses. Figure 1 shows an example of stimulation by a square pulse. The current profile depends on the electrode impedance and seal to the cell. Charge density can be evaluated, as shown by the third curve on this figure, by integrating current over time and dividing by the electrode active area ($400 \mu\text{m}^2$ in our case). The charge injection threshold is found to be $0.08 \mu\text{C}/\text{cm}^2$. This has been verified in ten different preparations. Depending on the time in culture, the threshold can vary by one order of magnitude. This value is nevertheless much lower than the threshold usually found for neural implants, such as the retinal [6], because of the controlled environment. Aiming at determining the lower baseline for neural prosthesis one can start by looking at the cultured cells thresholds.

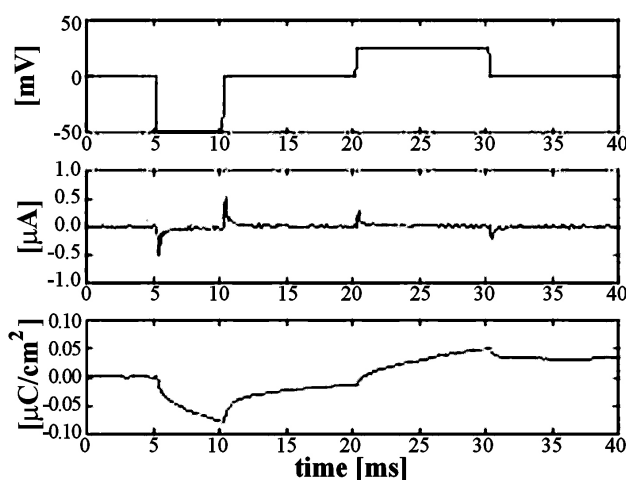


FIGURE 1. Charge injection tests.

4. Gas sensors based on nanomaterials

Nowadays there is an increasing interest in the monitoring and control of environmental conditions such as air pollution levels and hazardous gases. Thus, there is also an increasing demand for environmental monitoring by mean of selective, fast, compact, ease to operate, low cost systems. In this context, materials nanofabricated for sensing application that are compatible with integrated circuit technology can be a solution. Nanomaterials like PS have attractive characteristics such as a high specific area and high chemical surface activity. Nevertheless this material shows elevated sensitivity; properties such as selectivity and stability need to be improved, and it is important subject for research in the present, as discussed below.

5. Nano-composite of porous silicon for optical gas sensor application

Optical properties of PS can be used as an excellent material for the fabrications of photonic devices [7]. The high surface area of PS and their surface sensitivity to optical properties were used in order to fabricate the optical gas sensor [8]. Many efforts have been devoted to the elaboration of nano-composites based on PS. The objective could be to improve the electro luminescence efficiency, or also the realization of particular sensing properties [9].

In this work, the Photoluminescence (PL) behavior of thermal oxidized porous silicon/blue methylene (Ox-PS/BM) nano-composite, submitted to different organic ambients, was studied. Porous silicon (PS) layers were prepared by the electrochemical anodization method; after that, PS film was submitted to a thermal oxidation process in O_2 ambient at 900°C for 5 minutes. The Ox-PS surface was wetted with MB solution in ethanol; the solvent evaporation was obtained by spinning the wet sample (spin coating). The final Ox-PS/BM structure was analyzed by PL spectroscopy; the results of spectra indicated that MB molecules were adsorbed in the entire Ox-PS surface, conserving their monomer features, *i.e.* all the optical properties of BM molecules in low concentration organic solution were preserved.

The Ox-PS/BM structure was in the chamber vacuum (10^{-5} bar) initially, followed by the injection of organic gas vapor (benzene, methanol, butanol, hexane) and O_2 ambient respectively. A magnetic valve was used to control the gas injection into the vacuum chamber. The active open condition of the valve was obtained with an electrical pulse. For each electrical pulse, some gas concentration was injected into the chamber; this gas concentration was defined as one unit of an arbitrary scale for gas concentrations. Figure 2 (A) shows the PL emission of Ox-PS/MB after benzene vapor injection in the chamber; these intensities were normalized relative to PL intensity before gas injection as I/I_0 , where I represents the PL intensity after gas injection and I_0 represent the intensity before gas injection. Figure 2b shows the relative intensity spectra for benzene gas injection.

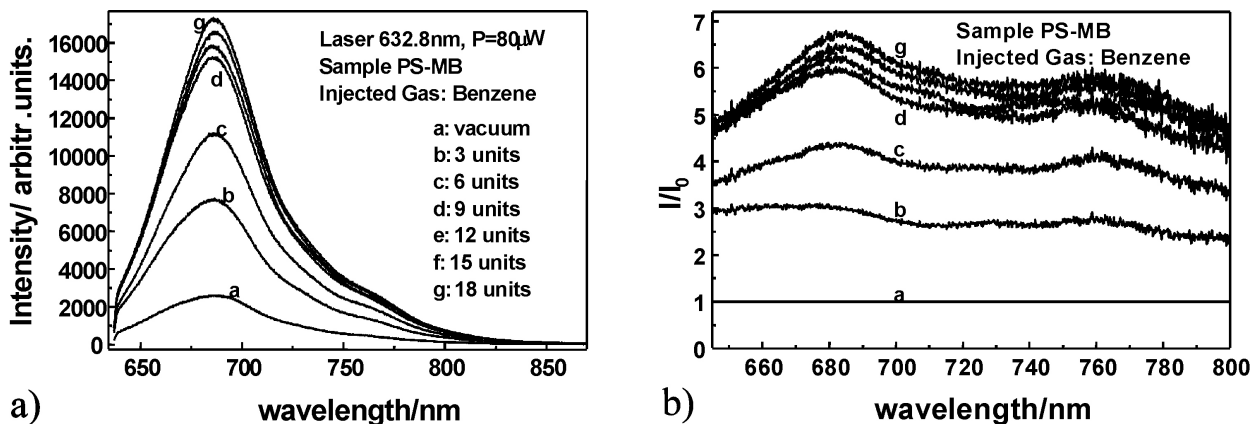


FIGURE 2. a) PL spectra of Ox-PS/MB film before and after benzene vapor injection at different concentrations, as indicated in the inside of figure. b) The relative intensity (I/I_0) spectra at different gas concentrations. The I and I_0 are the PL intensities after and before gas injection respectively. The line “a” corresponds to the reference spectrum (before gas injection).

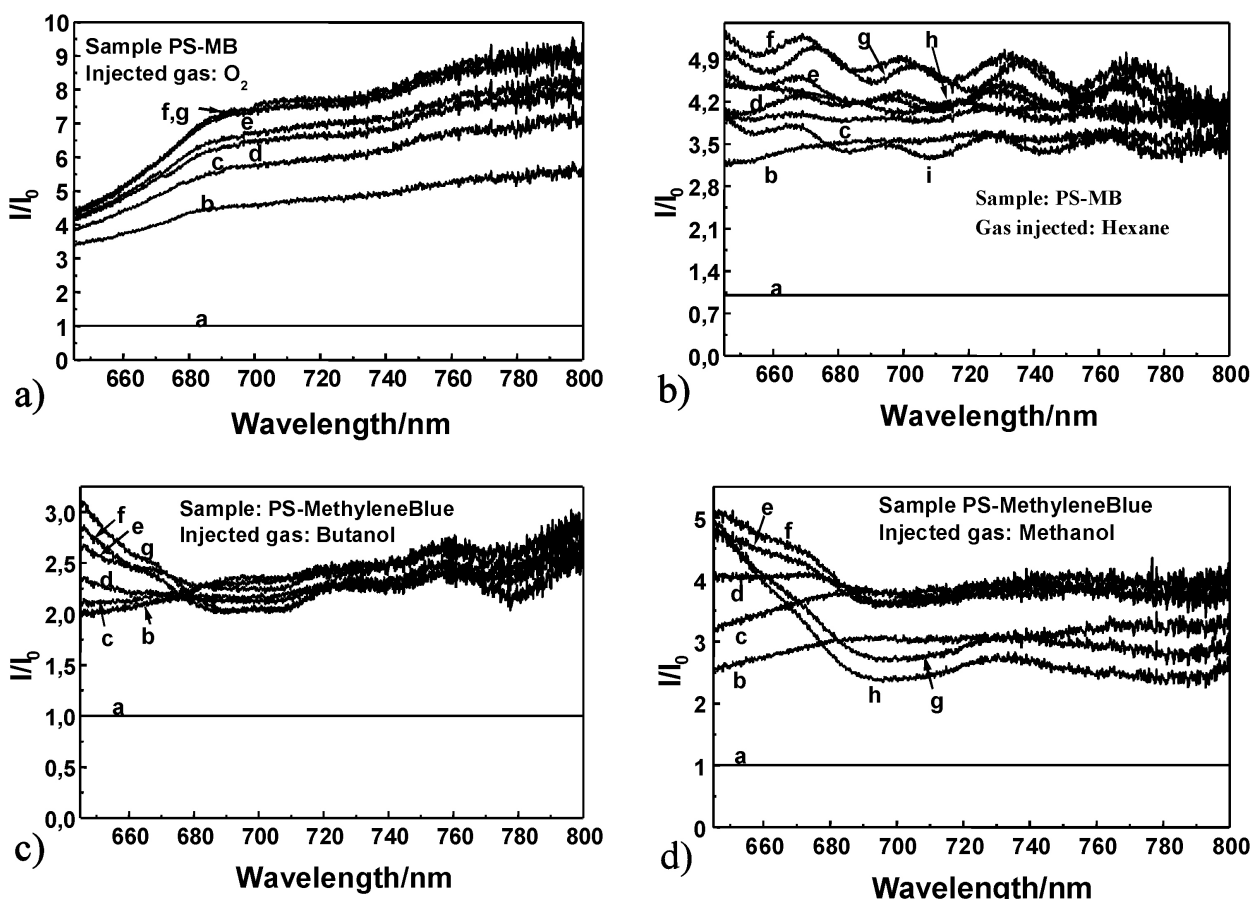


FIGURE 3. The relative intensity (I/I_0) spectra after the PS-MB film exposed to a) oxygen b) hexane c) butanol and d) methanol vapors. The I and I_0 are the PL intensities after and before gas injection respectively. Line “a” corresponds to reference spectrum (before gas injection). The color sequence b, c, d, e, etc, indicates the increase in gas concentration.

In the same way, the relative PL intensities were obtained for the O₂, hexane, butanol and methanol vapors, as can be seen in the Figs. 3a to 3d.

From the Figs. 2 and 3, it can be seen that the PL emission increased after gas injection in all cases. These behaviors can be explained as follows: the gas molecules adsorbed at

the Ox-PS/MB surface promote the cavity, which prevented the non-radiative recombination of excited state in the MB molecules, thus increasing the quantum efficiency of the radiative recombination.

For the O₂ and benzene vapor, the PL increased monotonically with the increase in gas concentration showing a

maximum sensibility near the peak of the PL band (680 nm); the lowest sensibility was observed at high energy spectrum region (< 680 nm), as can be seen in Figs. 2b and 3a. PL Intensity saturation was observed at 10 units of gas concentration in both O₂ and benzene vapors. The spectral response in the hexane vapor showed a monotonic increase in intensity from the low to intermediate vapor concentration (0 to 35 units), and a decrease was observed in the region of high vapor concentration (> 35 units), as can be seen in Fig. 3b.

In the case of butanol and methanol molecules, the high sensitivity of PL changing was observed in the high-energy region of PL spectra with their minimum at the PL peak position. In the low energy region the PL intensity showed the early saturation effect; in the case of butanol vapor, this effect appeared at 3 units of gas concentration, and in the methanol vapor, at 15 units of gas concentration. The PL intensity showed a slow decreasing effect at high vapor concentration in butanol vapor; in the case of methanol the PL decrease was more pronounced but their intensities were maintained at high values with respect to reference spectra (Fig. 3c and 3d). From the relative intensity spectra in the O₂ and benzene vapor a red shift in the PL band maximum could be observed (Low sensibility at high energy region, see Figs. 2b and 3a). These results suggest that the des-localization effect on the electrons in the MB molecules, which are responsible for the radiative emission, increases. However, the PL intensities showed the highest values in relation to butanol and methanol vapor. In the case of these last molecules, the PL band maximum were blue shift (high sensibility in the high energy region – see Figs. 3c and 3d suggesting that the electrons in the aromatic ring are more localized. It is worth considering in this case that butanol and methanol molecules have a high dipole moment ca. 1.7 Deybes.

From the above discussion and the behaviors of the relative intensity spectra, one might suggest that Ox-PS/MB film

can be used as an excellent optical gas sensor, which can be implemented in an optical system as an optical nose after a principal component analysis and pattern recognition obtained from the relative intensity spectra.

6. Conclusions

Some integrated sensors such as MEA and gas sensors based on nanomaterials were discussed.

With primary neuronal cultures developed over MEA, it is possible to maintain cells in a very well controlled environment, without the need for glial cells or high-resolution microscopy. We moreover show that the charge injection limit can be lowered to less than 100 nC/cm², which is helpful in determining thresholds for *in vivo* electrical stimuli in several neural prosthetic devices. Electrical stimulation of identified cells was also shown, and two stimulus-driven responses were presented: inhibitory stimuli and beating behavior.

The sensing mechanism of PS can be based on optical properties, as analysed in this paper. The PS film can be used as a good host material in order to obtain silicon organic dye molecules nano-composites. The Methylene Blue molecules were absorbed at the PS surface in the monomer structure conserving their optical properties (PL emission). The PL emission increases as the concentration of vapor gases increase, suggesting that the vapor promotes a cavity formation which could blind the MB molecule from the non-radiative ways. Finally, the relative intensity spectra showed the possible use of this film in optical nose fabrication.

Acknowledgment

WJS would like to thank FAPESP

1. T. Sauter, H. Nachtnebel, *IEEE Transactions on Inst. and Measurement*, **52**, (2003) 1854.
2. M.P. Maher et al., *Med. Biol. Eng. Comp.*, **37**, (1999) 110.
3. N.I. Syed, A.G.M. Bulloch and K. Lukowiak. *Science*, **283**, (1990) 282
4. N.L.V. Peixoto, S. Cordoba de Torresi, F.J. Ramirez-Fernandez, F.J. in: *Proceedings of BIOSIGNAL 2000*, Brno, Czech Republic, (2000) 86.
5. A. Stett, et al.. *Vision Research*, **40**, (2000) 1785
6. V. Parkhutik, *Solid State Electronic*, **43**, (1999) 1121.
7. W. J. Salcedo, F. J. Ramirez- Fernandez, J. C. Rubim, *Spectrochim. Act. A* **60**, (2004) 1077
8. L. T. Canham, *Appl. Phys. Lett.* **63**, (1993) 337.